Sustainable Food Technology

ROYAL SOCIETY OF CHEMISTRY

PAPER

View Article Online
View Journal

Cite this: DOI: 10.1039/d6fb00128a

High-molecular-weight chitosan as a sustainable structuring agent for olive oil oleogels: toward healthier and greener food systems

Álvaro Mosquera, [a] Leticia Montes, [a] Carlos A. Pena, [b] María López-Pedrouso, [c] Jorge Sineiro [d] and Daniel Franco *[e]

This study investigates, for the first time, the formulation and physicochemical properties of oleogels structured with high-molecular-weight chitosan (HMW-CH, 2439 kDa) through Schiff-base crosslinking. The objective was to evaluate the potential of HMW-CH as an oleogelator while emphasizing its economic and environmental advantages, since avoiding depolymerization reduces reagent use, energy consumption, processing time, and overall production costs, contributing to improved sustainability. Oleogels were prepared *via* an emulsion-templated method using olive oil and varying both the chitosan concentration (0.8 and 1.0%) and oil-to-water (O/W) ratio (60/40 and 50/50). Initially, aldehyde selection was performed based on drying kinetics and oil binding capacity, identifying 4-hydroxybenzaldehyde as the most suitable crosslinker. Microscopy and rheological analyses of emulsions, followed by structural, rheological, textural, thermal, and oxidative characterization of oleogels, were conducted to elucidate structure–property relationships. Significant correlations between emulsion properties, microscopy, and oleogel rheology suggested predictive potential for formulation design. Oleogels exhibited predominant gel-like behavior ($G' > G''$) across strain and frequency sweeps, confirming a stable three-dimensional network. The higher chitosan concentration (1%) significantly increased viscoelastic moduli, while the O/W ratio showed minor effects. A downward shift in chitosan T_{max} to ~270 °C indicated reduced thermal stability due to polymer–matrix interactions. Oleogels showed high oil binding capacity (86–88%), with no major dependence on the chitosan concentration or O/W ratio, although a significant interaction ($p = 0.008$) suggested synergistic effects on network stabilization. Hardness ranged from 1.22 to 1.54 N, with the O/W ratio exerting a moderate but significant influence ($p = 0.05$), aligning with textural requirements for spreadable products. Peroxide values remained low (<21 meq O_2 per kg), attributed to the drying process, and chitosan exerted a significant effect ($p < 0.0001$) in reducing primary oxidation. Digestibility tests showed decreased lipid hydrolysis compared with pure olive oil, suggesting that the dense chitosan network restricts enzymatic access to the oil phase. Overall, this study demonstrates that HMW-CH is a promising and sustainable structuring agent capable of producing oleogels with stable networks, desirable textural properties, and enhanced oxidative and digestive resistance, supporting their potential use as functional fat substitutes or controlled-release matrices.

Received 18th April 2026
Accepted 12th May 2026

DOI: 10.1039/d6fb00128a

rsc.li/susfoodtech

Sustainability spotlight

This work supports sustainable food systems by replacing saturated and trans fats with olive oil-based oleogels that improve lipid profiles while preserving food functionality. The direct use of high-molecular-weight chitosan avoids energy- and resource-intensive depolymerization steps, reducing costs, waste, and environmental impact. The proposed formulation strategy contributes to healthier, more economically and environmentally sustainable fat alternatives for processed foods.

[a]*Department of Chemical Engineering, Universidade de Santiago de Compostela, Santiago de Compostela, 15782, Spain*

[b]*CRETUS, Department of Chemical Engineering, Universidade de Santiago de Compostela, Santiago de Compostela, 15782, Spain*

[c]*Institute for Research in Global Health and Sustainable Development, iTERRA, Department of Biochemistry and Molecular Biology, Universidade de Santiago de Compostela, Lugo, 27002, Spain*

[d]*Aquatic One Health Research Center, iARCUS, Department of Chemical Engineering, Universidade de Santiago de Compostela, Santiago de Compostela, 15782, Spain*

[e]*Institute for Research in Global Health and Sustainable Development, iTERRA, Department of Chemical Engineering, Universidade de Santiago de Compostela, Santiago de Compostela, 15782, Spain. E-mail: daniel.franco.ruiz@usc.es*

1 Introduction

High intake of saturated (SFA) and trans (TFA) fats is linked to elevated cardiovascular disease risk. Accordingly, dietary guidelines from the WHO recommend limiting the consumption of SFA and TFA.[1] Although unsaturated fats from oilseeds provide a healthier option, their inclusion in processed foods remains challenging, because of the importance of these fats within the food industry. Oleogels from vegetable oils offer a solution by replicating the physical functionality of SFA/TFA, preserving sensory quality while improving lipid profiles.[2] Virgin olive oil, rich in favorable fatty acids and polyphenols, exhibits antioxidant and anti-inflammatory activity and is associated with reduced risk of diabetes, osteoporosis, and neurodegenerative diseases.[3]

Polysaccharides are promising oleogelators because their high molecular weight enables gelation at low concentrations; food-grade biopolymers can form oleogels *via* emulsion templating.[4] Among them, chitosan—obtained by chitin deacetylation—stands out for its biocompatibility, biodegradability, and chemical versatility. Most studies use low-molecular-weight chitosan (LMW-CH) due to its greater solubility and lower viscosity, which ease processing.[5] In contrast, high-molecular-weight chitosan (HMW-CH) with the molecular weight higher than 2000 kDa is scarcely explored in oleogels, despite its longer chains potentially enhancing the viscoelasticity, mechanical resistance, and gel strength.[6] Moreover, economically, HMW-CH is advantageous because many production routes yield high molecular weights initially; avoiding depolymerization to produce LMW-CH reduces reagent use, energy consumption, processing time, and waste, improving process sustainability.[7] Indeed, there are differences in prices between HMW-CH sourced for food/industrial applications, typically quoted at ~€8–30 kg^{-1}, and LMW-CH intended for cosmetic/pharmaceutical use, in the range ~€25–100 kg^{-1} (ref. 8). Additionally, recent market analyses project the global chitosan industry to grow at a ~12–20% CAGR through 2030.[9] Therefore, developing applications that can utilize HMW-CH directly, without the need for depolymerization, contributes to lower overall production costs and enhances the economic sustainability of the process. Additionally, the origin of chitosan should also be considered. Although chitosan derived from fungal sources has been reported to offer potential advantages over crustacean-derived chitosan,[10] it should be noted that commercial chitosan production is still predominantly based on crustacean shell waste. In this context, crustacean processing generates an abundant by-product stream worldwide, estimated at approximately 6–8 million tonnes annually. By contrast, no directly comparable global estimate is currently available for fungal biomass specifically suitable for chitosan production, as fungal sources remain more fragmented and are typically associated with specific fermentation side streams rather than a single large waste stream.[11]

Chitosan oleogels commonly rely on Schiff-base chemistry between chitosan amino groups and aldehyde carbonyls, forming imine crosslinks that generate oil-entrapping networks. Aldehyde identity critically determines the reactivity, crosslink stability, network flexibility, and compatibility with oil phases, thereby shaping the texture, viscosity, and stability. Aromatic aldehydes (*e.g.*, vanillin, syringaldehyde, *etc.*) often afford more stable linkages and stronger gels,[12,13] while aliphatic aldehydes can lead to more flexible networks, which may be advantageous in fine-tuning the rheological behavior of the oleogel. Although vanillin is widely employed as a cross-linker and a natural flavouring agent, its comparatively high price motivates evaluation of lower-cost alternatives, notably benzaldehyde and 4-hydroxybenzaldehyde. The cross-linking strategy itself does not preclude food applications; instead, suitability depends on the regulatory and toxicological acceptability of the compounds used in the final material. Since chitosan and 4-hydroxybenzaldehyde have precedents for approval or safety recognition in food-related contexts, this supports the potential use of the developed cross-linked system in food-industry applications.

Investigating HMW-CH for the first time in the context of oleogel formation is therefore scientifically justified, as it could reveal new physicochemical behaviors and improved structural characteristics not achievable with lower molecular weights. Therefore, the primary objective will be selecting a proper aldehyde for the Schiff reaction, and a secondary goal is to evaluate the effect of chitosan concentration (0.8 and 1.0%) and the oil-to-water (O/W) ratio (60/40 and 50/50) on the formulation of olive oil oleogels as well as the key oleogel properties, including emulsion stability, rheological and textural behavior, oil retention capacity, oxidation level and digestibility.

2 Materials and methods

2.1 Materials

HMW-CH from shrimp shells (79% DD, 1325 mPa s), benzaldehyde (BH), vanillin (VA), and 4-hydroxybenzaldehyde (4H) were supplied by Sigma Aldrich Inc. (St. Louis, MO, USA). Glacial acetic acid (≥99.7%), ethanol (96% v/v) and sodium acetate (≥90%) were provided by PanReac AppliChem (Monza, Italy). Virgin olive oil with acidity percentage less than 1% (Aceites Abril, Ourense, Spain) was acquired from a supermarket.

2.2 Characterization of chitosan

2.2.1 Determination of moisture and impurity content of chitosan. To achieve maximum accuracy in the amount of chitosan (CH) used in each of the emulsions, water and impurity content were calculated according to Mosquera *et al.*[14] Moisture content and impurities of the chitosan achieved were 10.92 ± 0.7% and 1.27 ± 0.1%, respectively.

2.2.2 Determination of viscosimetric molecular weight of chitosan. The average viscosimetric molecular weight (M_v) was determined by viscosity measurements, using a Ubbelohde type viscometer (AVS 350, Schott-Geräte GmbH, Germany) equipped with a thermostatic bath with stirring (J. P. Selecta, Digiterm 100, Barcelona, Spain) to maintain a constant temperature of 25 °C ± 0.1 °C during the test. Two types of properly calibrated

capillary tubes were used (Xylem Analytics Germany GmbH, I or 0C, Washington DC, USA).

The chitosan solution (1 g L^{-1}), was prepared over a total period of 24 h. Half of the required chitosan was initially added and dissolved at 70 °C under constant stirring at 500 rpm for 1 h. The remaining chitosan was then added and dissolved under the same conditions for a further 1 h. After 2 h of dissolution, the temperature was decreased to 50 °C, while stirring was maintained at 500 rpm until the 24 h preparation period was completed. After dissolution, the solution was filtered to remove insoluble impurities. The final chitosan concentration was subsequently corrected based on the measured impurity content, as the viscometric determination is highly sensitive to small changes in sample concentration. To facilitate filtration of the viscous chitosan solution, the temperature was increased to 70 °C during the first 15 min of the filtration step.

Five dilutions were performed (0.0032, 0.0064, 0.0097, 0.012 and 0.016 g dL^{-1}), and five replicates along with buffer and the stock solution at 1 g L^{-1} were also analyzed. The stock solutions of chitosan were prepared in a specific solvent, which is related to the constants of the Mark–Houwink, eqn (1). Specifically, values for constants were selected from the methodology proposed by Rinaudo *et al.*,[15] which indicates the use of acetic acid buffer (0.3 M)/sodium acetate (0.2 M) and values of $K = 0.076$ and $\alpha = 0.76$

$$[\eta] = K \times M_v^{\alpha} \quad (1)$$

where K (dL g^{-1}) and α (dimensionless) parameters, known as viscometric constants, are associated with the relationship between the solvent used and the polymer studied, as well as the physicochemical properties of the latter. The intrinsic viscosity was obtained using the Huggins and Kraemer equations and the Fedors equation, following the methodology described by Montes *et al.*[16]

2.3 Elaboration of oleogels

2.3.1 Preparation of solutions. The protocol used was based on previous studies[12,13] with slight modifications. To produce the emulsion, chitosan (5% w/w acetic acid), comprising the continuous (aqueous) phase, and an aldehyde solution in ethanol 96% were used. The chitosan dissolution protocol was previously described in Section 2.2.2. After preparation, the pH was measured to confirm if it was below 6. The amount of chitosan prepared in each solution varied depending on the desired final concentration in the oleogel; meanwhile, the amount of aldehyde used in the oleogel formulation was predetermined by the amount of chitosan added, maintaining a ratio of 1.3 mol of aldehyde per mol of chitosan in all cases.

The chitosan concentration in the solutions was adjusted according to the target final concentration in the oleogel and the O/W ratio specified in the experimental design. The required concentrations ranged from 0.98% to 1.82%, corresponding to formulations with 0.8% chitosan and an O/W ratio of 50 : 50, and 1% chitosan and an O/W ratio of 60 : 40, respectively.

2.3.2 Preparation and drying of emulsions. Preparation of emulsion was carried out according to the protocol of Mosquera *et al.*[14]. Emulsions (90 g) were dried in a convective dryer (ACS Angelantoni, Challenge 250, Massa Martana, Italy) following the methodology proposed by Lama *et al.*[17] Briefly, emulsions were placed in Petri dishes in a uniform 1.2 mm-thick layer. The thickness of the emulsion layer in the dish is a critical parameter during drying. To obtain the data required for studying the drying kinetics of emulsions with different aldehydes, a gravimetric method was applied during drying. One of the two sample plates was alternately removed from the dryer every 5 minutes and weighed. The first measurement was taken 7 minutes after introducing the plates into the dryer to ensure steady-state conditions. The successive weight data allowed determining the evolution of the emulsions' moisture content over time. After one hour of drying, measurements were taken every 30 minutes since the drying rate slowed down. Drying conditions were set at 70 °C with 10% relative humidity and an air speed of 2 m s^{-1}. Drying was carried out for a total of 3 h, until the moisture content, calculated according to eqn (2), was below 2%.

$$X(\%) = \frac{m_i - m_i(1 - W)}{m_s} \times 100 \quad (2)$$

where m_i is the mass of emulsion at a given time i, m_s is the theoretical dry mass of emulsion i and W is the mass fraction of volatile components in the emulsion (water, acetic acid, and ethanol). For this calculation, the amount of oil that could volatilize was disregarded, as it is practically negligible at the drying temperature (70 °C).

Once the desired drying level was reached, emulsions were removed from the dryer and wrapped in a plastic film to prevent moisture absorption from the environment. Emulsions were left to rest for 24 hours before the grinding stage, at room temperature and in the absence of light, to avoid possible oil oxidation. The grinding step was carried out solely to reduce the bulk oleogel into smaller, more manageable fragments for storage, rather than to generate a new microstructure. Therefore, it was performed as gently as possible to minimize disturbance of the pre-formed oleogel network, in accordance with the approach reported by Mosquera *et al.*[14]

2.4 Analytical methodology

2.4.1 Microscopy analysis of emulsions. An optical microscope (Zeiss, Axioskop 40, Jena, Germany) equipped with a 20 MP digital camera (Kern Optics ODC 841, Ebingen, Germany) was employed to capture the images. Optical magnifications of 10× and 20× were used on an emulsion sample placed on a sample holder, covered with a coverslip and observed under direct illumination.

The emulsion samples were studied twenty-four hours after preparation. To obtain a representative study for each emulsion, six samples were analyzed, and a total of four photographs per sample was taken. The images obtained were processed using ImageJ software (version 1.54p, NIH, Bethesda, MA, USA), splitting color channels to analyze the green color component

and adjusting the threshold. The parameters obtained were the average Feret diameter, the drop average area and the number of retained drops per mm^2.

2.4.2 Rheological analysis. A stress-controlled rheometer (Physica MRC 301, Anton Paar, Graz, Austria) equipped with RheoCompass™ software was used to characterize the rheological properties of the oleogels. Measurements were carried out with a parallel-plate geometry (50 mm diameter) at 25 °C, with temperature control ensured by a Peltier system (±0.01 °C) combined with a thermostatic bath (Ecoline Staredition E 100, Lauda, Germany). The plate gap was adjusted to 1 mm for emulsions and 1.5 mm for oleogels. To avoid the loss of volatile components (water, acetic acid, and ethanol) during emulsion measurements, the sample periphery was sealed with paraffin. The linear viscoelastic region (LVR) was initially established by an amplitude sweep from 0.01% to 10% strain at a constant frequency of 1 Hz. Afterwards, a frequency sweep from 0.1 to 100 Hz was conducted at 0.1% strain to assess the viscoelastic behavior of the samples.

2.4.3 Thermogravimetric analysis. The thermogravimetric behaviour of oleogel samples was investigated using a TA Instruments Q500 thermogravimetric analyser. High-purity nitrogen (99.999%, Nippon Gases) served as both the balance and sample purge gases, delivered at flow rates of 40 mL min^{-1} and 60 mL min^{-1}, respectively. Each oleogel specimen was placed in an open platinum crucible, which was then automatically transferred into the furnace chamber. The thermal program consists of heating from ambient temperature to 600 °C at a constant rate of 10 °C min^{-1}. Mass changes were continuously recorded, and the resulting thermogravimetric curves were processed and interpreted using the Universal Analysis 2000 software package (TA Instruments).

2.4.4 Textural profile analysis of oleogels. Texture profile analysis (TPA) was conducted with a texture analyzer (TA.XT-plus, Stable Micro Systems, Surrey, UK). For each experimental condition, three oleogel samples (5 g each) were molded as cylinders (∅ 19.5 mm). A 25 mm aluminum probe (P/25) performed two consecutive compression cycles to 50% strain. Crosshead speeds were 2 mm s^{-1} (pre-test), 1 mm s^{-1} (test), and 2 mm s^{-1} (post-test). The trigger force was set at 0.1 N, and force–time curves were recorded. From these curves, maximum hardness (N), cohesiveness (dimensionless), springiness (mm), and adhesiveness (N s) were calculated.

2.4.5 Oil binding capacity of oleogels. The oil-binding capacity (OBC) was determined following Morales *et al.*[18] with minor modifications. Approximately 1 g of each oleogel was placed into pre-weighed 2 mL microcentrifuge tubes (Eppendorf-type). Samples were centrifuged (HW12 and HWLAB, LinHai, China) at 13 500 g for 25 min at ambient temperature. The tubes were then inverted for 10 min to drain unbound oil, the supernatant was carefully removed with a Pasteur pipette, and the residues were reweighed. The OBC (%) was calculated using eqn (3)

$$\mathrm{OBC} = \left[1 - \left(\frac{m_1 - (m_2 - m)}{m_1}\right)\right] \times 100 \quad (3)$$

where m is the mass of the empty Eppendorf tube, m_1 is the mass of the tube containing the oleogel before centrifugation, and m_2 is the mass of the tube after centrifugation and removal of the supernatant oil.

2.4.6 Colour parameters of oleogels. Color was measured using a portable colorimeter (CR-400, Konica Minolta, Osaka, Japan). The instrument was calibrated against a white ceramic standard ($L^* = 92.60$, $a^* = 0.3133$, and $b^* = 0.3195$) prior to use. All measurements were performed 24 h after oleogel preparation, and samples were equilibrated to room temperature for 15 min before testing. The results were expressed in the CIELAB space as lightness (L^*), redness (a^*), and yellowness (b^*). Chroma (C^*) and hue angle (h^*) were calculated using eqn (4) and (5), respectively.

$$h^* = \tan^{-1}\left(\frac{b^*}{a^*}\right) \quad (4)$$

$$C^* = \sqrt{a^{*2} + b^{*2}} \quad (5)$$

2.4.7 Primary and secondary oxidation analyses. Oil was first recovered from the oleogels by centrifugation at 9576 × g for 20 min. Primary oxidation was then assessed by the peroxide value (PV) following the AOCS methodology.[19] Briefly, 0.3–0.5 g of oil was dissolved in chloroform, followed by sequential addition of glacial acetic acid, distilled water, and potassium iodide; the liberated iodine was titrated with an automatic titrator (HI901 Color, Hanna Instruments, Woonsocket, RI, USA). The results were expressed as milliequivalents of oxygen per kilogram of oil (meq O_2 per kg). Secondary oxidation was evaluated by the thiobarbituric acid reactive substances (TBARS) assay using a modified protocol from Zhao *et al.*[20] In brief, 0.5 g of oleogel was mixed with reagent containing 2% (w/w) HCl, 0.375% (w/w) thiobarbituric acid, and 15% (w/w) trichloroacetic acid. Mixtures were incubated in a water bath at 95 °C for 15 min, cooled to ambient temperature for 15 min, and filtered through a 0.45 μm membrane. Absorbance was measured at 532 nm on a UV spectrophotometer (GENESYS 10, Thermo Spectronic, Menlo Park, CA, USA). TBARS were quantified against a 1,1,3,3-tetraethoxypropane calibration curve and expressed as mg of malondialdehyde (MDA) per kilogram of oil.

2.4.8 Lipid digestibility of the oleogels. The *in vitro* digestion procedure followed the INFOGEST protocol[21] with slight modifications, which are described in Mosquera *et al.*[14] As controls, it used pure olive oil and an olive-oil oleogel prepared with LMW-CH at 1%. The percentage of free fatty acids (FFA%) released during digestion was determined from the volume of NaOH consumed during titration, using eqn (6). The calculation assumes that lipase hydrolyzes two free fatty acids per triglyceride molecule, as described by Li and McClements.[22]

$$\mathrm{FFA}(\%) = \frac{V_{\mathrm{NaOH}} \times M_{\mathrm{NaOH}} \times MW_{\mathrm{lipid}}}{2 \times W_{\mathrm{lipid}}} \times 100 \quad (6)$$

where V_{NaOH} is the volume (L) of NaOH used to neutralize the released fatty acids, M_{NaOH} is the molarity (M) of the NaOH solution, MW_{lipid} is the average molecular weight of the triglycerides (879.67 g mol^{-1}), and W_{lipid} is the total lipid mass (g) in the sample.

2.4.9 Experimental design and statistical analysis. Analysis of variance (ANOVA) using the general lineal model (GLM) procedure of the SPSS package (SPSS 25.0, Chicago, IL, USA) was performed for the oleogel physicochemical traits studied. The fixed effect of CH concentration and O/W ratio was included in the model (eqn (7)).

$$Y_{ij} = \mu + \mathrm{CH}_i + \mathrm{O/W}_j + \mathrm{CH} \times \mathrm{O/W}_{ij} + \varepsilon_{ij} \quad (7)$$

Here, Y_{ij} is the observation of the dependent variable, μ is the overall mean, CH_i is the effect of chitosan concentration, $\mathrm{O/W}_j$ is the effect of oil in water ratio $(\mathrm{CH} \times \mathrm{O/W})_{ij}$ is the interaction term of chitosan concentration and oil in water ratio and ε_{ij} is the residual random error associated with the observation.

Based on the experimental moisture content data over time, the drying behavior of the oleogels was fitted using three classical thin-layer drying models: Newton, Henderson–Pabis, and Page, expressed, respectively, by the following eqn:

$$\text{Newton: } MR = \exp(-kt) \quad (8)$$

$$\text{Henderson–Pabis: } MR = a\exp(-kt) \quad (9)$$

$$\text{Page: } MR = \exp(-ktn) \quad (10)$$

where MR is the moisture ratio, defined by eqn (11) as:

$$MR = \frac{M_t - M_e}{M_0 - M_e} \quad (11)$$

with M_t representing the moisture content at time t, M_0 the initial moisture content, and M_e the equilibrium moisture content. The parameters k, a, and n are empirical constants specific to each model and drying condition. To evaluate the fit quality, the coefficient of determination (R^2), the goodness-of-fit coefficient (ϕ), and the root mean square error (RMSE) were calculated using the following eqn:

$$R^2 = 1 - \frac{\sum \left(MR_{exp} - MR_{pre}\right)^2}{\sum \left(MR_{exp} - \overline{MR}_{exp}\right)^2} \quad (12)$$

$$\phi = \frac{\sum \left(MR_{exp} - \overline{MR}_{exp}\right)\left(MR_{pre} - \overline{MR}_{pre}\right)}{\sqrt{\sum \left(MR_{exp} - \overline{MR}_{exp}\right)^2 \sum \left(MR_{pre} - \overline{MR}_{pre}\right)^2}} \quad (13)$$

$$\mathrm{RMSE} = \sqrt{\frac{1}{N}\sum_{i=1}^{N}\left(MR_{pre,i} - MR_{exp,i}\right)^2} \quad (14)$$

where MR_{exp} and MR_{pre} denote the experimental and predicted moisture ratios, respectively, and N is the number of observations.

3 Results and discussion

3.1 Characterization of HMW-chitosan

The characterization of the gelling agent employed is essential, since its behaviour greatly influences the properties of the oleogels. To obtain the molecular weight (M_v) using a viscosimetric method, work is required on dilute regime, defined as the range of concentrations where the polymer molecules behave independently.[23] In the case of CH, this is particularly important because it behaves as a polyelectrolyte in solution, where electrostatic repulsion forces can induce a deformation of the typical rod-like structure of polysaccharides, thereby modifying their hydrodynamic volume and consequently affecting the results of viscometric studies.[24] To verify that the dilutions prepared for the viscometry experiments were within the dilute regime, the linear relationship between the variations in viscosity and the solution concentration was confirmed (Fig. SI 1A), indicating no interactions among the molecules that could modify the hydrodynamic volume and alter the final outcome of the viscometry. The intrinsic viscosity $[\eta]$ could be obtained as the intersection of the linearized Huggins and Kraemer equations, where values of K' and K'' correspond to the slopes of each equation, respectively (Fig. SI 1B). The Fedors equation can be applied in both the dilute and semi-dilute regimes, with the only requirement being that the relative viscosities fall within the range of 1 to 100.[25] Using a linear regression, both the intrinsic viscosity $[\eta]$ (slope) and the limiting concentration (C_{max}, g dL^{-1}), before the onset of intermolecular interactions (y-intercept), were obtained (Fig. SI 1C).

The M_v values were calculated according to the Mark–Houwink equation for both methods (Huggins/Kraemer and Fedors) using constants K and α reported by Rinaudo *et al.*[15] according to the degree of deacetylation of the CH samples. For comparative purposes, three other commercial CHs were also measured. Our results confirm that the solvent used was appropriate, since in the studied systems there is strong solvent–polymer interaction and weak intermolecular interaction, inferred from the K' values lower than 0.5 and the negative K'' values (Table 1), in agreement with Montes *et al.*[16] Moreover, the difference between K' and K'' was less than 0.5 in both cases, which further indicates good chitosan solubilization and the solvent's ability to prevent intermolecular interactions due to its high polarity.[23] Indeed, there were no significant differences in the calculation of $[\eta]$ values obtained from both methods, which may be attributed to the high dilution degree. The M_v values calculated for each chitosan sample, together with their respective DD, provide an explanation for the marked differences in solubility between these polymers, despite being the same compound. For instance, the HMW-CH has a lower DD than LMW-CH (79% *vs.* 85%, respectively) and a higher molecular weight (2439 kDa *vs.* 204 kDa). These characteristics explain why HMW-CH exhibits poorer solubility than LMW-CH, a trend consistently reported in the literature. Indeed, several studies[15,26] concluded that increasing DD improves solubility, whereas others[27,28] established a direct relationship between higher molecular weight and poorer solubility—a phenomenon also observed in the present study. For instance, according to Rinaudo,[15] when working with CH samples possessing optimal characteristics for good solubilization (low molecular weight, high DD, and derived from β-chitin), complete solubilization can be achieved simply by adding enough protons to the solution to balance the concentration of amino groups.

Table 1 Viscosimetric molecular weight of different chitosan samples[a]

	Huggins/Kraemer				Fedors		
	K'	K''	$[\eta]$ (dL g^{-1})	M_v (kDa)	C_{max} (g dL^{-1})	$[\eta]$ (dL g^{-1})	M_v (kDa)
β-CH	−0.5	−0.71	6.90	167	0.128	7.45	185
α-LMW-CH	0.171	−0.240	8.27	204	2.18	8.28	205
α-MMW-CH	0.166	−0.222	11.39	312	2.73	11.33	310
α-HMW-CH	0.176	−0.218	52.91	2439	0.561	52.14	2392

[a] β-CH was acquired by Glentham Life-Sciences from squid, whereas other commercial α-chitosans (LMW = low molecular weight, MMW = medium molecular weight and HMW = high molecular weight) were acquired by Sigma-Aldrich from shrimp.

3.2 Selection of aldehyde employed in the Schiff reaction

To determine which aldehyde is most suitable for the formulation of this type of oleogel, two critical criteria were selected: drying kinetics and oil binding capacity (OBC). The former is critical for assessing industrial applicability, as drying is one of the most energy-intensive unit operations. Moreover, previous studies by our research group on vanillin-crosslinked chitosan oleogels showed that oven-drying can preserve oil more effectively than freeze-drying and promote higher viscoelasticity, suggesting the formation of a denser and more interconnected network.[17] Although freeze-drying is advantageous for preserving thermosensitive compounds, it is considerably more energy-intensive, costly, and technically demanding. By contrast, oven-drying is simpler, more economical, and more operationally feasible at the industrial scale. In parallel, high OBC values are essential to meet the specifications required for classification as an oleogel.

Fig. 1 shows the evolution of moisture over time for oleogels containing 0.5% and 1% CH in the final product for the three selected aldehydes. After 2 hours, all oleogels had reached a moisture content below 3%, although the drying rates varied among them. Drying times increased with higher chitosan concentration: at 0.5% CH, BH, VA, and 4H reached the target moisture at 52, 85, and 47 min, respectively (Fig. 1A), whereas at 1% CH, drying times increased to 57, 90, and 90 min (Fig. 1B). These differences confirm a direct relationship between the increase in the CH concentration and the required drying time in agreement with Lama *et al.*[17]

A higher CH concentration led to the formation of a more extensive and complex network, resulting in stronger retention of the aqueous phase and greater resistance to diffusion toward the surface, thereby hindering evaporation from the solid phase. Another phenomenon observed was the formation of a dry oleogel crust caused by the initial evaporation of surface water, which reduced the drying rate. This effect is reflected in the drying curves: the initial moisture drop shows a steep slope, but as the crust thickens and hardens over time, it restricts water diffusion through the emulsion, slowing evaporation and

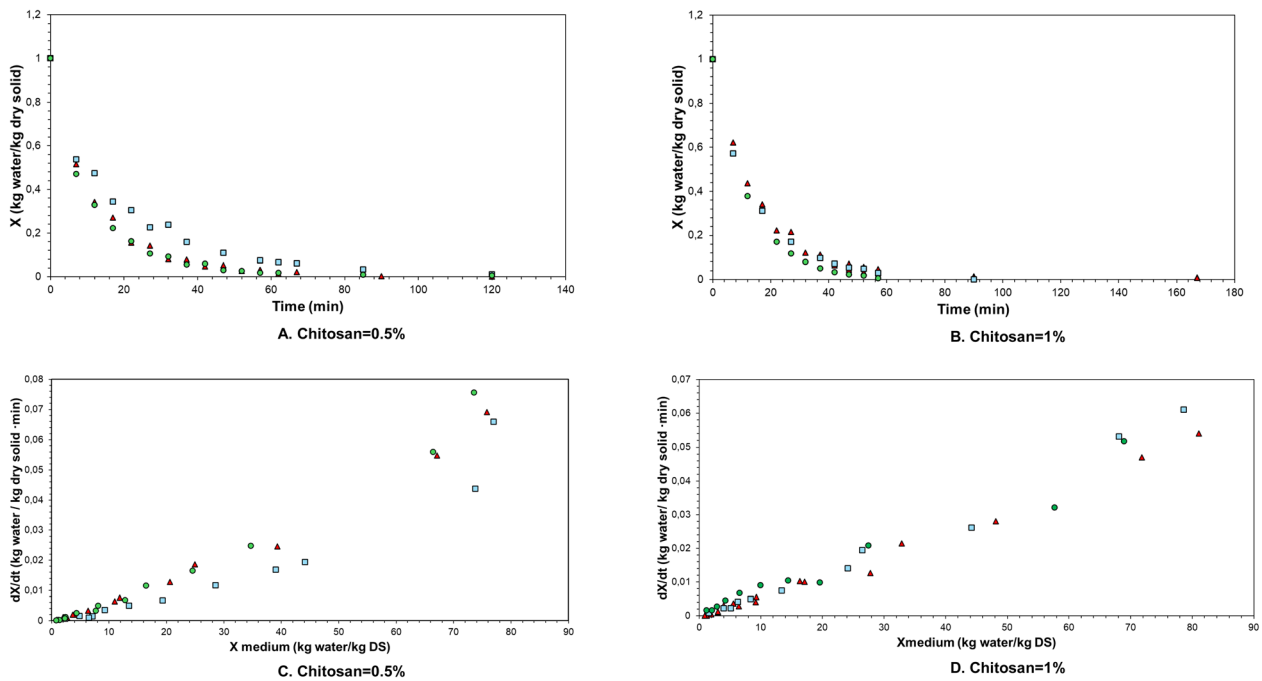

Fig. 1 of moisture *versus* time for oleogels with CH = 0.5% (A) and CH = 1% (B) and drying rate *versus* mean moisture for oleogels with CH = 0.5% (C) and CH = 1% (D). Red triangle: benzaldehyde; blue square: vanillin; green circle: 4-hydroxybenzaldehyde.

Table 2 Drying rate constant for each system studied and statistical parameters R^2, φ, and RMSE for the Henderson Pabis, Page and Newton models

Henderson Pabis model						
	CH	K (s^{-1})	a	R^2	φ	ECM
BH	0.5%	0.001338	0.9763	0.9943	114.10	0.018
	1.0%	0.001102	1.0375	0.9939	153.58	0.020
VA	0.5%	8.62×10^{-4}	0.9235	0.9743	71.7107	0.034
	1.0%	$1.18 \cdot 10^{-3}$	1.0377	0.9937	45.2428	0.020
4H	0.5%	1.46×10^{-3}	0.9737	0.9936	98.9919	0.019
	1.0%	1.33×10^{-3}	0.9992	0.9999	5467.37	0.0018
Page model						
	CH	K (s^{-1})	n	R^2	φ	ECM
BH	0.5%	0.0046	0.8242	0.9982	582.6329	0.008425
	1.0%	0.00137	0.9636	0.9932	162.945	0.01914
VA	0.5%	0.00811	0.7002	0.9950	473.240	0.0141
	1.0%	0.00160	0.9500	0.9939	24.3965	0.0159
4H	0.5%	0.00654	0.7840	0.9994	973.524	0.0050
	1.0%	0.00146	0.9866	0.9999	5799.574	0.0015
Newton model						
	CH	K (s^{-1})		R^2	φ	ECM
BH	0.5%	0.001369		0.9949	108.61	0.018
	1.0%	0.001061		0.9924	147.09	0.020
VA	0.5%	0.000942		0.9783	55.95	0.038
	1.0%	0.001128		0.9924	34.99	0.020
4H	0.5%	0.001494		0.9944	90.95	0.019
	1.0%	0.00083		0.9977	205.21	0.014

producing a more gradual decline (Fig. 1A and B). This phenomenon is further intensified by the reaction between amine and aldehyde groups. As the reaction proceeds, a progressively more rigid three-dimensional network forms through multiple covalent linkages and additional hydrogen bonds. This structural reinforcement reduces molecular mobility and hinders water evaporation. Consequently, the differences observed in drying kinetics among the oleogels can be attributed to variations in network development, with VA-containing formulations showing the slowest drying rates compared with those prepared using 4H or BH. This effect is especially pronounced in oleogels with 0.5% CH (Fig. 1A).

To study this phenomenon more rigorously, Fig. 1C and D present the drying rate (dX/dt, kg water per kg dry solids per min) as a function of moisture content. Karaer and Kaya,[29] using scanning electron microscopy, confirmed that the product of a Schiff base reaction exhibits a structure composed of porous layers with a smooth surface. These pores are presumed to be the main pathways through which water diffusion occurs during the drying process. This suggests that the reaction between CH and aldehyde, along with the nature and extent of the reaction product, generates structural differences that can either facilitate or hinder water migration during drying, consequently influencing oil entrapment. During the drying of oleogels containing 0.5% CH (Fig. 1C), the drying rate was found to be lower when VA was used, consistent with the formation of a more compact molecular network compared to that formed with 4H or BH. This denser molecular arrangement limits water diffusivity relative to that observed with the other two aldehydes. The formation of this compact network is attributed to additional hydrogen bonding involving free functional groups. After reacting with CH *via* the primary Schiff base mechanism, VA has a hydroxyl and a methoxy group capable of forming hydrogen bonds with similar groups or with amino groups.[30] Similarly, 4H can establish hydrogen bonds through its single free hydroxyl group after the reaction,[31] although the overall reaction extent is lower, as reported by several studies,[29,32] wherein maximum conversions of 63% for VA and 59% for 4H were observed in systems comparable to the present study. Therefore, the drying of oleogels prepared with 4H is expected to proceed faster than those formulated with VA. In contrast, BH lacks any free functional group capable of forming hydrogen bonds with the CH chain after reaction, resulting in the weakest network among the three systems studied, but there were no significant differences between oleogels prepared with 4H and BH (Fig. 1C). For oleogels containing 1% CH (Fig. 1D), the drying kinetics showed no appreciable difference. This could be attributed to the higher CH concentration, which leads to a more compact network structure that is less dependent on the extent of the reaction, thereby inherently reducing the drying rate. These results demonstrate that it is possible to obtain stable oleogels using lower concentrations of gelling

agent, provided the reaction is properly monitored to ensure stabilization of the CH molecular network through hydrogen bonding, particularly when using aldehydes bearing free hydroxyl groups after Schiff base formation, such as VA and 4H. Although in all cases the emulsions could be dried in less than two hours, achieving a residual moisture content below 3%, the samples were kept in the drying oven for up to three hours. This was done in accordance with Marin *et al.*,[31] who reported that Schiff base reactions reach their maximum conversion after approximately two hours in the absence of water, with reaction progress being further promoted at elevated temperatures.

Drying kinetic data were modelled (Table 2). All models exhibited R^2 values greater than 0.97, indicating excellent agreement between experimental and predicted data and confirming the suitability of these models to describe the drying kinetics of the oleogels. Among the systems analyzed, the formulation containing 4H at a CH concentration of 1% showed the best correlation (highest ϕ) between experimental and predicted data, while the corresponding system prepared with VA displayed the poorest fit, regardless of the model used. Consistently, the lowest RMSE value was obtained for the oleogel containing 4H at the highest CH concentration, further supporting its superior predictive agreement. Regarding model comparison, the Newton model yielded the lowest R^2 and ϕ values, followed by the Henderson–Pabis and Page models, in that order. A similar trend was observed in the RMSE values, which were highest for the Newton model and lowest for the Page model across all systems. Nevertheless, these differences were not statistically significant, suggesting that the increased complexity and parameterization of multi-parameter models may not be justified for explaining the drying kinetics of these oleogel systems.

The second criterion for aldehyde selection was the OBC due to its critical importance. For oleogels prepared with a CH concentration of 0.5% (Fig. 2), the use of 4H yielded the highest OBC value (70%), followed by BH (54%) and VA (29%). The oleogel formulated with VA collapsed during centrifugation, releasing a substantial amount of entrapped oil. This phenomenon could be attributed to an excessive extent of reaction that could produce an overly rigid molecular network, resulting from the numerous hydrogen bonds formed between the free hydroxyl and methoxy groups in VA. Such rigidity hindered oil entrapment due to the lack of flexibility within the molecular structure, a behavior also reported by Xu *et al.*[30] When the CH concentration was increased to 1%, the same trend was observed: the system prepared with 4H again exhibited the highest OBC value, followed by VA, and finally BH. The oleogel produced with BH also experienced structural collapse during centrifugation, like the VA system at lower CH concentrations. In this case, the collapse may be explained by the combination of a higher CH concentration and the low reaction extent characteristic of BH, approximately 13%,[30] along with the structure of HMW-CH, which due to its long and poorly cross-linked chains was unable to form an effective three-dimensional structure between chitosan and BH, thereby exhibiting weak oil retention.

None of the oleogels studied reached an OBC value higher than 90%, although a clear increasing trend was observed with the higher CH concentration. It can therefore be concluded that both an excessively high or insufficient reaction extent between CH and aldehyde reduce the OBC, either by inducing excessive rigidity or by preventing efficient molecular crosslinking. From this perspective, the use of 4H appears most advantageous, as it promotes the formation of hydrogen bonds that effectively crosslink the molecular network while maintaining sufficient flexibility to trap and retain oil. Moreover, 4H also led to faster drying kinetics. This feature is highly relevant because drying is one of the most energy-demanding unit operations on the industrial scale.

Although residual free aldehyde was not directly quantified in this study, the aldehyde-to-amine ratio was selected to be stoichiometric with respect to the available amino groups of chitosan, making a significant excess of unreacted aldehyde unlikely. Nevertheless, further analytical work is needed to quantify residual aldehyde and evaluate the stability of the

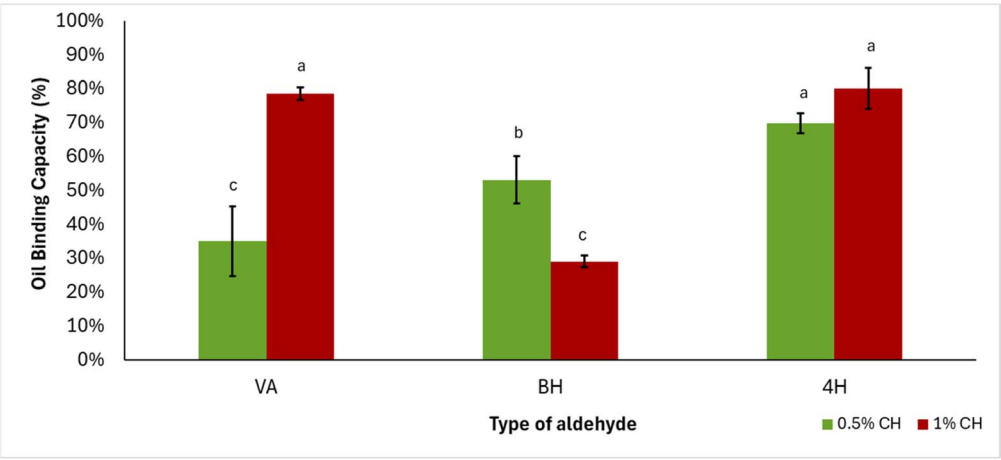

Fig. 2 OBC for oleogels with two chitosan concentrations (0.5 and 1%) for each aldehyde (VA, BH and 4H). Different letters (a, b, and c) mean significant differences among mean values according to the Duncan test.

Image/Parameter	System 1	System 2	System 3	System 4
	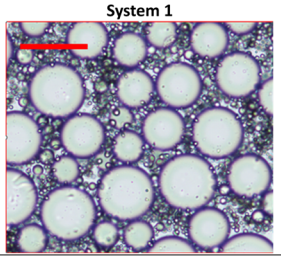	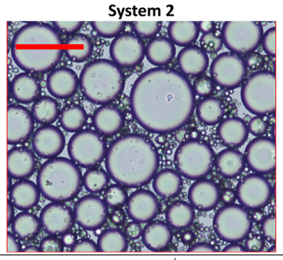	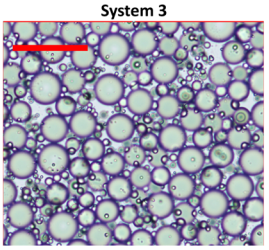	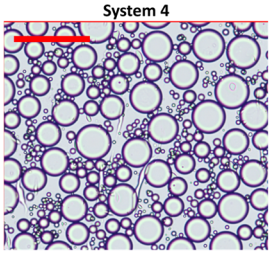
ND (drops/mm^2)	338.5±68^c	697±58.70^b	1,133±80.60^a	1,078±117^a
Average Feret Diameter (μm)	39.0±3.30^a	29.2±2.90^b	20.7±1.40^c	19±0.70^c
Average particle size(μm^2)	1318±314^a	697±104^b	339±68^c	290.9±17.6^c

Fig. 3 Optical microscopy images of emulsions employed and morphological features (number of drops; average Feret diameter and average particle size). System 1 (0.8% CH and 60/40 O/W); system 2 (1.0% CH and 60/40 O/W); system 3 (0.8% CH and 50/50 O/W); system 4(1.0% CH and 50/50 O/W); red bar = 100 microns. Different superscripts mean significant mean differences at 95% level confidence.

imine linkages under application-relevant and gastrointestinal conditions.

Therefore, considering not only OBC and drying kinetics but also sensory properties, cost, volatility, and the potential risk of residual aldehyde after processing, 4H was identified as the most suitable aldehyde for the experimental formulations and was consequently selected for further experimental design, particularly because it is expected to have a less pronounced sensory impact than vanillin, although any assumption regarding its more efficient removal during drying should be interpreted cautiously and ideally verified experimentally.

3.3 Microstructural and rheological characterization of emulsions

No studies in literature have reported the use of CH with the M_w employed in this study (2439 kDa). This M_w is unusually high, as commercially available chitosans typically fall within the 4–200 kDa range, and indeed Mun *et al.*[33] refer to CH with a M_w of 200 kDa as a high molecular weight. To achieve a stable system with 1% HMW-CH and the highest O/W ratio (*e.g.* [CH]: 1%; O/W: 60/40), it is necessary to slightly change the experimental conditions to avoid aggregation, hence the emulsification process was shortened to 3 minutes for this system.

Results from microscopical observation (droplet number, Feret diameter and average size) are shown in Fig. 3, highlighting that all systems exhibited a bimodal droplet-size distribution, with most of the oil content present in larger droplets. Emulsions from systems 3 and 4 differed significantly from the other two (systems 1 and 2), as their average droplet size was significantly smaller (Fig. 3A–D). For emulsions prepared at a 50/50 O/W ratio, no statistical differences ($p > 0.05$) were observed among the three evaluated morphological parameters. The CH concentration did not influence oil droplet size measured as the Feret diameter. In contrast, a significant effect of CH concentration on droplet size was observed for emulsions prepared with the highest oil content (*e.g.* 60/40 O/W ratio), with droplets formed using 1% chitosan being slightly larger (29.2 ± 2.90 μm) than those obtained with 0.8% chitosan (39.0 ± 3.30 μm). Moreover, these oil droplets were substantially larger than those reported by Mosquera *et al.*,[14] who used LMW-CH and reported droplet sizes in the range of 4–8.5 μm. The number of droplets per mm^2 significantly decreased with the O/W ratio, in accordance with the decrease of the Feret diameter (Fig. 3), in contrast with the results previously reported employing LMW-CH.[14]

In addition to the differences in degree of polymerization between the two types of chitosan, the HMW-CH used in this study had a lower degree of deacetylation, resulting in a higher proportion of hydrophobic non-acetylated residues. These non-acetylated units are likely to adsorb onto the surface of the dispersed phase during the initial stages of the emulsification process.[34] Such adsorption reduces the interfacial tension, which in turn promotes the formation of larger oil droplets. Payet & Terentjev[35] also hypothesized that a higher CH concentration in an emulsion leads to a decrease in the interfacial tension, since the non-deacetylated monomers absorbed onto the surface of the dispersed phase will hinder the phase contact, requiring an increase of the surface contact area and, therefore, increasing the droplet size under similar stress conditions.

Strain sweep tests (Fig. 4A) were performed on chitosan-based emulsions to identify their linear viscoelastic regime and assess the evolution of the storage (G') and loss (G'') moduli as a function of strain. For most formulations, G remained higher than G'', indicating a predominantly elastic network. Increasing the chitosan concentration (from 0.8% to 1.0%) led to higher values of both G' and G'', reflecting a more structured and elastic system. However, in the least structured emulsion (CH = 0.8% 50/50 O/W), G'' values were consistently greater than G' across much of the strain range, demonstrating a predominance of viscous behavior. This suggests that low polymer content and lower oil phase limit the formation of a stable network, leading to a primarily dissipative response typical of weak or poorly structured emulsions.[36]

Fig. 4B presents the frequency sweep results for the emulsions. As seen in the strain sweep, increasing the CH concentration (with a constant O/W ratio) resulted in higher moduli and more pronounced elastic character. In contrast, the emulsion with lower CH concentration and lower oil content (CH = 0.8% 50 : 50) again exhibited $G'' > G'$ throughout the frequency range, confirming the dominance of viscous behavior.[37]

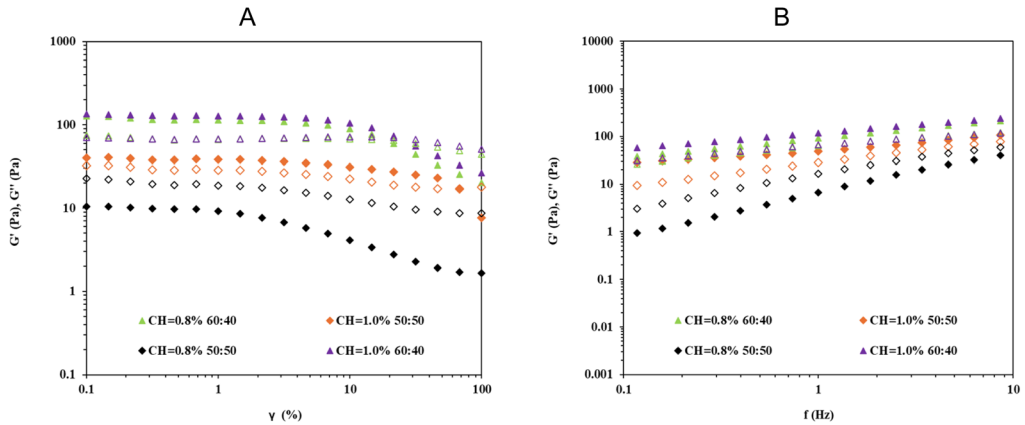

Fig. 4 Rheological profiles of emulsions: (A) strain sweep from 0.1% to 100% strain at 1 Hz and (B) frequency sweep from 0.1 to 10 Hz at 1% strain. Filled symbols denote G', while open symbols correspond to G''.

In addition, significant correlations were found between the viscoelastic parameters and the emulsion composition. Both G' and G'' of the emulsions showed strong positive correlations with the oil/water ratio ($p < 0.01$; $r = 0.781$ and $r = 0.828$, respectively), indicating that formulations with higher oil content develop more structured networks with greater elastic and viscous responses.[38] Moreover, a significant negative correlation was observed between the viscous modulus G'' of the emulsions and the number of droplets ($p < 0.05$; $r = -0.634$), suggesting that systems with fewer, likely larger or more strongly flocculated droplets exhibit higher energy dissipation under oscillatory shear, which is consistent with the formation of more continuous, viscous-dominated structures.[39] In addition, the damping factor ($\tan\delta = G''/G'$) showed a significant negative correlation with chitosan concentration ($p < 0.05$; $r = -0.608$), indicating that increasing polymer content leads to relatively more elastic and less dissipative emulsions.

Based on the observations of the present study, a 60/40 O/W ratio can be considered the upper limit for the preparation of oleogels containing 1% or higher concentrations of HMW-CH.

3.4 Rheological characterization of oleogels

Strain sweep tests were carried out to determine the linear viscoelastic region (LVR) of the oleogels. Fig. 5A shows the evolution of the storage (G') and loss (G'') moduli as a function of strain, where all samples exhibited a gel-like response, with G' remaining higher than G'' over most of the strain range, in agreement with previous observations for emulsion-templated oleogels.[40] Oleogels formulated with the highest CH concentration displayed the greatest values of G' and G'', reflecting a stronger and more elastic network, which can be attributed to the higher density of polymer chains and intermolecular interactions that reinforce the three-dimensional structure.[41]

Fig. 5B shows the frequency sweep results of the oleogels for all studied systems. In all cases, the storage modulus (G') remained higher than the loss modulus (G'') throughout the entire frequency range, indicating the predominant elastic (gel-like) nature of these oleogels. This behavior, a higher G' than G'' in frequency sweeps of chitosan gels, has been widely reported and confirms the formation of a stable three-dimensional network.[42] Increasing the CH concentration from 0.8% to 1.0% resulted in significantly higher modulus values,

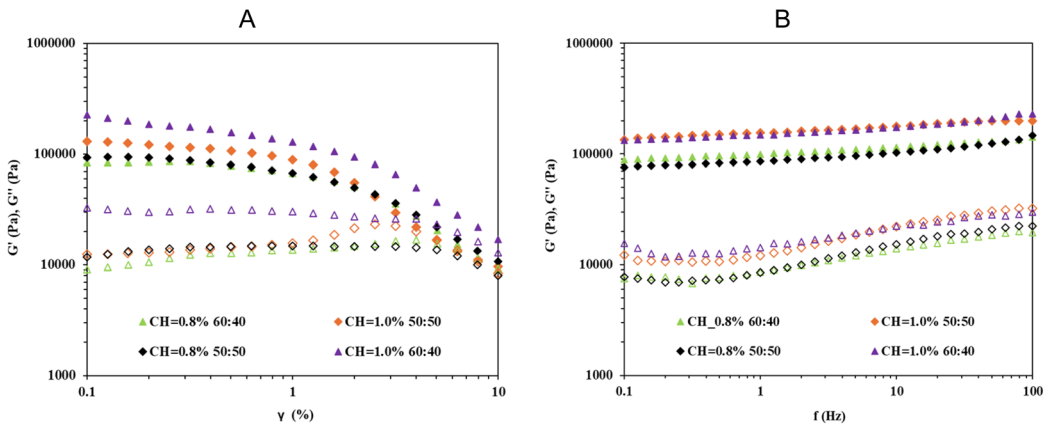

Fig. 5 Rheological profiles of the oleogels: (A) strain sweep from 0.1% to 10% strain at 1 Hz and (B) frequency sweep from 0.1 to 100 Hz at 1% strain. Filled symbols denote G', while open symbols correspond to G''.

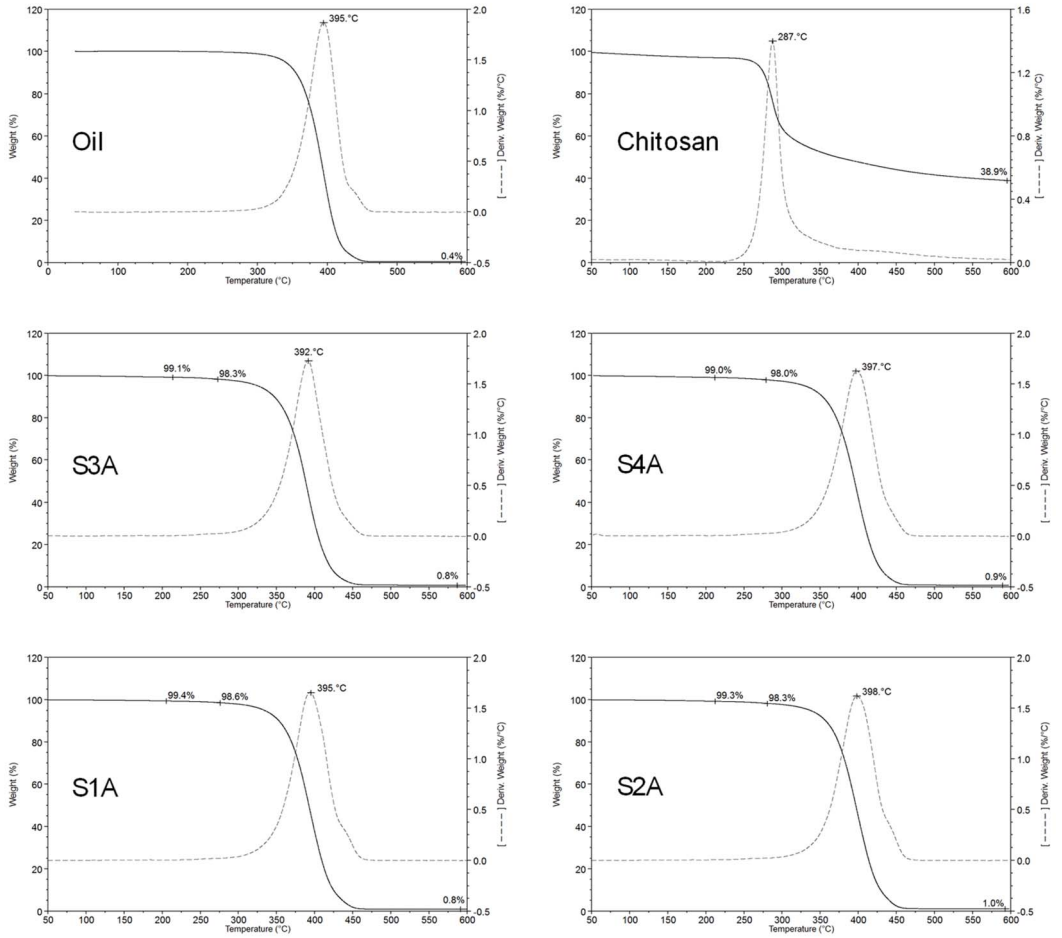

Fig. 6 TGA curves of the olive oil oleogels elaborated with two different HMW-CH concentrations and two O/W ratios. S1A (0.8% CH, 60/40 O/W); S2A (1.0% CH, 60/40 O/W); S3A (0.8% CH, 50/50 O/W); S4A (1.0% CH, 50/50 O/W).

demonstrating that a denser polymer network yields more rigid and cohesive structures, in agreement with prior rheological studies of CH matrices. In contrast, modifying the O/W ratio produced only minor differences when the CH content was kept constant, indicating that the viscoelastic properties are mainly governed by the CH concentration under these conditions.[43] Moreover, significant correlations were found between the viscoelastic properties of the emulsions and those of the corresponding oleogels, with G' and G'' of the oleogels showing positive correlations with the G' and G'' values of the emulsion ($p < 0.05$; $r = 0.598$ and $r = 0.654$, respectively). This suggests that the rheological behaviour of the final oleogel can be anticipated from measurements performed at the emulsion stage, which is highly relevant for formulation design and process optimisation.

3.5 Thermal stability of oleogels

TGA of pure CH yields a substantially larger residual mass at 600 °C than the oil (Fig. 6). CH leaves a residue of 38.9%, while olive oil leaves 0.4%. These residues are primarily associated with non-volatile fractions such as inorganic salts and mineral compounds that are expected in CH but absent in oil. Thermal decomposition behaviour was assessed through the peaks identified in the first-derivative thermogravimetric (DTG) curves, which indicate the temperature at which each component reaches its maximum rate of mass loss (T_{max}). For the pure compounds, T_{max} values were determined to be 395 °C for olive oil and 287 °C for CH. In the oleogel samples, the T_{max} of CH is not clearly distinguishable due to overlap with the decomposition peak of the oil. However, as reported for LMW-CH,[14] its T_{max} consistently shifts to lower temperatures, averaging *c.a.* 270 °C. This downward shift suggests a reduction in its thermal stability, likely influenced by interactions within the matrix or formulation-related factors.

The T_{max} of oil remains largely consistent at 395 °C ± 3 °C, indicating that its thermal behavior is not significantly influenced by the presence of other components. The percentage of mass loss observed at each decomposition stage closely aligns with the relative amounts of chitosan and oil in the formulations, reflecting their distinct thermal contributions. Notably, no signs of water evaporation were detected prior to thermal breakdown, suggesting that water was not retained within the oleogel matrix under the experimental conditions.

Upon complete thermal degradation, the residual mass at 600 °C is related to the chitosan content in each oleogel. As shown in the thermogram of pure CH, it is the dominant source of high-temperature residue due to its composition rich in non-volatile inorganic matter. Therefore, the remaining mass after decomposition serves as a reliable indicator of the chitosan proportion within the oleogel formulation.

3.6 Physicochemical and oxidative properties of oleogels

The evaluation of physicochemical attributes and oxidative stability is essential to determine the performance of oleogels intended for food applications (Table 3). Color parameters (L^*, a^*, and b^*) may provide insights into the visual quality and potential consumer acceptance, particularly when evaluating alternatives to conventional fat. The color parameters of the oleogels were notably influenced by both the CH concentration and O/W ratio. L^* increased slightly with higher CH content and greater O/W ratio, suggesting that formulations containing more oil during the emulsion process or more CH appeared somewhat lighter. This effect was statistically significant for both the CH concentration ($p = 0.001$) and the O/W ratio ($p = 0.047$), with a highly significant interaction ($p < 0.0001$). However, none of the oleogels exhibited pronounced brightness (*i.e.* $L^* < 50$) according to Barragán-Martínez *et al.*[44] Regarding the coordinatesa^* and b^*, they were positive in all oleogels, indicating a reddish and yellowish hue in agreement with a previous study.[14] The yellow index was predominant, as the b^* coordinate was approximately 7–10 times higher than that of a^* The behavior of b^* was significantly affected by the O/W ratio ($p < 0.0001$). The higher the oil content in the emulsion, the more intense the yellow tone of the oleogel. There was a significant interaction effect between the CH concentration and O/W ratio ($p < 0.0001$), with higher values observed at O/W = 60, indicating a more pronounced yellow hue. This interaction suggests that the yellow tone increases at O/W ratios with higher oil content when the chitosan concentration is high, but at O/W ratios with more water content, the b^* yellow index increases with the lower CH concentration compared to its respective experimental point with the higher CH concentration. Finally, hue was significantly affected by both the CH concentration ($p = 0.016$) and O/W ratio ($p < 0.0001$), reflecting perceptible shifts in the overall hue across the oleogel formulations; meanwhile, color saturation (C^*) followed the same trend as b^*, with greater saturation observed at O/W = 60.,

Overall, the O/W ratio emerged as the most influential factor in determining color characteristics, particularly for b^* and C^*, while CH exerted a smaller yet statistically significant effect on L^* and h^*. The color differences observed among oleogels are likely associated with variations in their molecular network structures, resulting from changes in the gelling agent concentration and emulsification conditions. These variations lead to different degrees of crosslinking, suggesting non-uniform reaction extents across formulations, as previously reported.[13,30]

OBC is a key parameter that reflects the ability of an oleogel to immobilize liquid oil within its network. High OBC values—ideally 90% or greater—are desirable to minimize oil leakage during storage and handling, thereby ensuring effective oil entrapment, structural integrity, and overall product stability. In the present study, values for all oleogels were high (86–88%) and did not vary significantly with either chitosan ($p = 0.435$) or the O/W ratio ($p = 0.768$). The absence of a statistical effect of CH concentration may be attributed to the narrow concentration range tested (0.8–1%). Moreover, the complexity of working with HMW-CH is reflected in the variability of the results (*i.e.* high standard deviation). In line with this, the interaction CH × O/W ratio was significant ($p = 0.008$), suggesting that the specific combination of both factors may exert a slight influence. It was not possible to obtain an OBC ≥ 95%, indicating

Table 3 Effect of the chitosan concentration and O/W ratio on physicochemical parameters (color, OBC, textural parameters and oxidation level) of olive oil oleogels

	Chitosan concentration		O/W ratio		Significance p-value		
	0.8%	1.0%	50	60	Chitosan	O/W	CH × O/W
Color parameters							
L^*	32.96 ± 3.01	35.47 ± 4.28	33.61 ± 2.29	34.82 ± 5.00	0.001	0.047	<0.0001
a^*	1.94 ± 0.66	1.98 ± 0.33	2.36 ± 0.23	1.56 ± 0.32	0.718	<0.0001	0.012
b^*	12.84 ± 0.55	12.77 ± 4.34	11.01 ± 2.41	14.60 ± 2.36	0.831	<0.0001	<0.0001
h^*	1.42 ± 0.04	1.39 ± 0.07	1.35 ± 0.03	1.46 ± 0.01	0.016	<0.0001	0.016
C^*	13.06 ± 0.54	12.95 ± 4.24	11.26 ± 2.39	14.76 ± 2.29	0.704	<0.0001	<0.0001
OBC (%)	86.23 ± 5.04	88.14 ± 6.39	87.54 ± 4.28	86.83 ± 7.09	0.435	0.768	0.008
TPA parameters							
Hardness (N)	1.29 ± 0.52	1.49 ± 0.24	1.54 ± 0.35	1.22 ± 0.43	0.153	0.050	0.005
Springiness (mm)	0.54 ± 0.11	0.42 ± 0.12	0.53 ± 0.15	0.43 ± 0.08	0.117	0.156	0.996
Cohesiveness (%)	0.31 ± 0.02	0.28 ± 0.03	0.30 ± 0.03	0.29 ± 0.02	0.078	0.354	0.678
Adhesiveness (N s)	−0.40 ± 0.13	−0.43 ± 0.19	−0.43 ± 0.16	−0.40 ± 0.16	0.794	0.750	0.058
Oxidation level							
IP (meq O_2 per kg oleogel)	20.84 ± 1.04	17.59 ± 2.58	20.56 ± 1.44	17.87 ± 2.77	<0.0001	0.002	0.014
TBARS(μmol MDA per g oleogel)	0.45 ± 0.11	0.84 ± 0.19	0.92 ± 0.40	0.37 ± 0.03	<0.0001	<0.0001	<0.0001

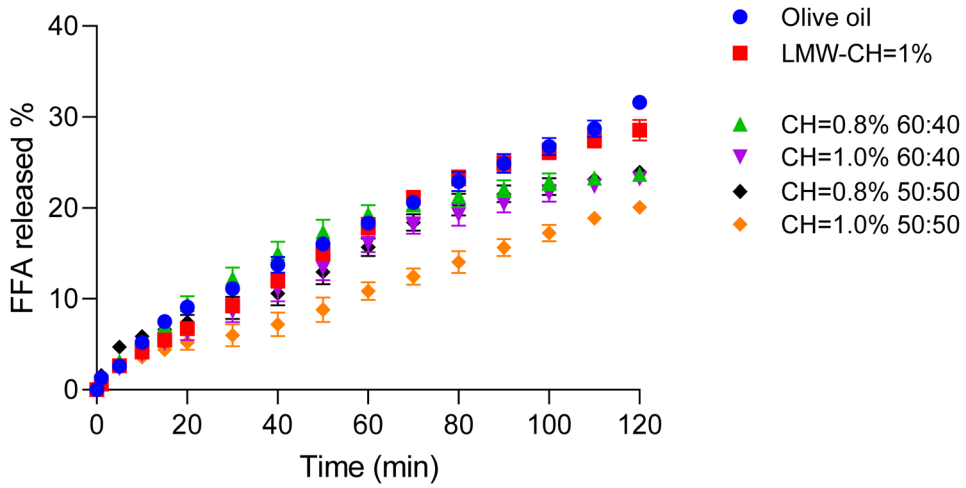

Fig. 7 Digestibility of olive oil and oleogels structured with chitosan. Effect of chitosan concentration and O/W ratio on total free fatty acids.

that none of the oleogels developed a highly stable molecular network, unlike those previously formulated with LMW-CH.[14,45]

The damping factor ($\tan\delta = G''/G'$) of the oleogels showed a significant positive correlation with OBC ($p < 0.05$; $r = 0.700$), indicating that systems with a more dissipative viscoelastic response tend to exhibit slightly higher oil retention under the conditions studied.

Texture analysis, typically assessed through hardness, cohesiveness, and elasticity, reflects the structural integrity of the oleogel network. These properties are strongly dependent on the gelator concentration and the interactions between the polymeric matrix and the oil phase. A well-structured oleogel should exhibit sufficient firmness to maintain shape while preserving spreadability, which is critical for applications such as fat replacers in bakery or confectionery products. Oleogels were obtained with hardness values ranging from 1.22 to 1.54 N, a narrower range compared to that observed in oleogels previously formulated with LMW-CH.[14] In the literature, textural analysis usually demonstrated that the gelator concentration strongly affected the hardness, but in the present study it cannot confirm this hypothesis. Oleogels formulated with the highest CH content exhibited higher hardness (1.49 *vs.* 1.29 $p = 0.153$), although it did not reach statistical significance. These findings are consistent with a denser three-dimensional network. In contrast, the O/W ratio exerts a moderate but significant effect, the hardness value increasing with the decrease of oil content in the emulsion (1.22 *vs.* 1.54 $p = 0.05$). This highlights the need for a deeper understanding of the O/W ratio, a variable that has been scarcely studied in the literature. The term interaction showed a significant interaction ($p = 0.005$), indicating that the combined effect of the studied factors plays a relevant role in hardness. Specifically, oleogels with an O/W ratio of 50 exhibited greater hardness. Concerning springiness, cohesiveness, and adhesiveness, there were no significant variations among oleogels ($p > 0.05$), suggesting that elasticity and cohesion are relatively insensitive to the evaluated factors. The G' and G'' values of the oleogels were negatively correlated with cohesiveness ($p < 0.05$; $r = -0.643$ and $r = -0.662$, respectively), indicating that stiffer, more elastic networks are associated with less cohesive structures in texture profile analysis, thus linking small-amplitude oscillatory measurements with large-deformation textural properties.[46]

According to these findings, HMW-CH oleogels may be suitable as substitutes for commercial spreadable products such as butter or margarine, which typically exhibit hardness values between 1.02 and 3.27 N. Although the oil-binding capacity values obtained in this study indicate substantial rather than complete oil immobilization and remain below those reported for the most highly structured oleogel systems, they are still consistent with functional edible oleogels and, together with the spreadable texture observed, support their potential application in spreadable or semi-solid fat-rich foods such as pâtés, creams, and related products.[47,48]

Oxidative stability was evaluated through primary oxidation markers (PV) and secondary oxidation products (TBARS). Low values indicate effective protection against lipid oxidation, which is crucial for maintaining nutritional quality and preventing off-flavors. Significant differences were found in both indicators as a result of the CH concentration and the O/W ratio and their interaction (Table 3). Oleogels prepared with a CH concentration of 1% and an O/W ratio of 60 showed a PV below the limit of 20 meq O_2 per kg of oil established by the European regulations for virgin olive oil.[49] Higher TBARS values were observed at an O/W ratio of 60 and at lower chitosan concentrations, partially consistent with the trends observed for PV. However, despite this tendency, TBARS levels remained low across all oleogels studied.

The relatively low peroxide values are likely attributable to a combination of factors, including the physical structuring of the oil within the gel network, which may act as a barrier to oxygen diffusion and thereby slow oxidation kinetics relative to bulk oils, as well as the intrinsic antioxidant and metal-chelating properties of chitosan,[50] rather than to a major contribution from free 4-hydroxybenzaldehyde, which has been reported to exhibit only limited or negligible antioxidant activity in some bulk-oil and radical-scavenging assays.[51] Moreover, it

should be emphasized that, although this aldehyde contains a phenolic group, it was primarily used as a reactive crosslinking agent for Schiff base formation. While its residual free concentration was not quantified in the present study, its residual level is expected to be low, as it was discussed in the drying section.

3.7 Oleogel digestibility

The results of oleogel digestibility are presented in Fig. 7. For comparative purposes, the digestibility of pure olive oil was assessed alongside that of an oleogel formulated with 1% LMW-CH. No significant differences ($p > 0.05$) were observed among the various oleogels, regardless of the CH concentration or O/W ratio, reaching an overall average digestibility value of 23.59 ± 0.36%, with the exception of the oleogel containing 1% CH and O/W ratio of 50/50, which exhibited a lower final digestibility value (20.07 ± 0.57%). At the end of the digestion process (120 min), the olive oil control exhibited the highest digestibility (31.62 ± 0.12%), followed by the oleogel formulated with LMW-CH (28.54 ± 1.14%). Examination of the digestion curves revealed that the differences among oleogels prepared with HMW-CH, LMW-CH and pure olive oil became evident after approximately 80 minutes of digestion.

These findings suggest that the oleogels undergo slightly slower digestion than pure olive oil, likely due to the structuring effect of chitosan, which forms a molecular network that restricts enzymatic access to the oil phase. The lower digestibility observed compared with oleogels formulated with LMW-CH[14] may further indicate that HMW-CH promotes greater structural integrity during digestion and increased resistance to enzymatic degradation. This behaviour could be advantageous in applications aimed at protecting bioactive compounds or promoting delayed release during gastrointestinal transit. However, the results should be interpreted as evidence of a modest modulation or slight delay of lipolysis, rather than a definitive proof of a fully established controlled-release mechanism, since other factors may also contribute to the observed behaviour, including matrix disintegration during digestion, incomplete oil release, chitosan-related interfacial effects, and differences in lipid accessibility. In this regard, previous studies have shown that chitosan may influence lipid digestion through aggregation phenomena, bile salt adsorption, and partial lipase suppression,[52,53] while the droplet size and interfacial composition are also recognized determinants of lipolysis kinetics.[54,55] Because these contributions were not independently quantified in the present study, the observed behaviour is more appropriately attributed primarily to structural hindrance, with possible secondary interfacial effects.

4 Conclusions

This study demonstrated for the first time that high-molecular-weight chitosan (2439 kDa) can be effectively employed to structure olive oil oleogels through Schiff-base crosslinking with 4-hydroxybenzaldehyde. Among the aldehydes evaluated, 4-hydroxybenzaldehyde proved to be the most suitable due to its ability to form hydrogen bonds that reinforce the chitosan network while maintaining sufficient flexibility, resulting in efficient oil immobilization and faster drying kinetics. The resulting oleogels exhibited high oil binding capacities (86–88%) and hardness values within the range of commercial spreadable fats, confirming their potential as functional fat replacers for the food industry. The oil-to-water ratio emerged as the most influential factor affecting both texture and color, while the chitosan concentration played a secondary role. Although none of the systems reached OBC values above 95%, the oleogels showed adequate structural integrity, thermal stability, and oxidative resistance. Furthermore, digestibility tests revealed that the use of high-molecular-weight chitosan reduced lipid hydrolysis compared with low-molecular-weight systems, suggesting greater structural persistence during digestion, which could be beneficial for controlled lipid release and protection of bioactive compounds. From a broader perspective, the use of high-molecular-weight chitosan represents a promising scientific advance in oleogel formulation and a potentially more sustainable alternative for food applications. By employing chitosan without prior depolymerization, the process reduces energy and chemical consumption, contributing to the development of more environmentally friendly and potentially economically viable fat-based systems. However, these findings should be interpreted within the exploratory scope of the present study, since the food use of chitosan is not yet broadly established across regulatory frameworks, particularly as a structuring agent for oleogel applications. Therefore, while the results highlight the technological potential of HMW-chitosan, further studies addressing safety, regulatory acceptance, scalability, and application-specific performance will be required before industrial implementation can be fully envisaged.

Author contributions

Conceptualization: M. L.-P. and D. F.; methodology: Á. M.; formal analysis: Á. M., L. M., C. A. P. and J. S.; investigation: Á. M., L. M., C. A. P. and J. S.; data curation: Á. M. and L. M.; writing – original draft preparation: M. L.-P. and D. F.; writing – review and editing: L. M., C. A. P., M. L.-P., J. S. and D. F.; visualization: M. L.-P.; supervision: D. F.; project administration: D. F.; funding acquisition: D. F. All authors have read and agreed to the published version of the manuscript.

Conflicts of interest

The authors declare no conflicts of interest.

Data availability

The data supporting the findings of this study are available from the corresponding author upon reasonable request.

Supplementary information (SI) is available. See DOI: https://doi.org/10.1039/d6fb00128a.

Acknowledgements

This work was funded by MCIN/AEI/10.13039/501100011033 and, as appropriate, by the European Union Next Generation EU/PRTR (grant CNS2022-135217). Daniel Franco and Jorge Sineiro were supported by ED431B 2024/18, a Grupo de Potencial Crecimiento funded by Xunta de Galicia (Spain).

References

1 A. N. Reynolds, L. Hodson, R. De Souza, H. T. D. Pham, L. Vlietstra and J. Mann, *Saturated Fat and Trans-fat Intakes and Their Replacement with Other Macronutrients: a Systematic Review and Meta-Analysis of Prospective Observational Studies*, World Health Organization, Geneva, Switzerland, 2023.

2 M. López-Pedrouso, J. M. Lorenzo, B. Gullón, P. C. B. Campagnol and D. Franco, Novel strategy for developing healthy meat products replacing saturated fat with oleogels, *Curr. Opin. Food Sci.*, 2021, **40**, 40–45, DOI: 10.1016/J.COFS.2020.06.003.

3 E. Yilmaz and Ş. Demirci, Preparation and evaluation of virgin olive oil oleogels including thyme and cumin spices with sunflower wax, *Gels*, 2021, **7**, 95, DOI: 10.3390/gels7030095.

4 H. Qiu, H. Zhang and J. B. Eun, Oleogel classification, physicochemical characterization methods, and typical cases of application in food: a review, *Food Sci. Biotechnol.*, 2024, **33**, 1273–1293, DOI: 10.1007/s10068-023-01501-z.

5 R. Román-Doval, S. P. Torres-Arellanes, A. Y. Tenorio-Barajas, A. Gómez-Sánchez and A. A. Valencia-Lazcano, Chitosan: properties and its application in agriculture in context of molecular weight, *Polymers*, 2023, **15**, 2867, DOI: 10.3390/polym15132867.

6 H. C. Yang and M. H. Hon, The effect of the molecular weight of chitosan nanoparticles and its application on drug delivery, *Microchem. J.*, 2009, **92**, 87–91, DOI: 10.1016/J.MICROC.2009.02.001.

7 B. Bellich, I. D'Agostino, S. Semeraro, A. Gamini and A. Cesàro, The good, the bad and the ugly of chitosans, *Mar. Drugs*, 2016, **14**, 99, DOI: 10.3390/md14050099.

8 *Chitosan, Chemondis Online Database*, accessed 2025, https://chemondis.com/substance/chitosan/.

9 Mordor Intelligence, *Chitosan market report*, Mordor Intelligence, accessed 2025, https://www.mordorintelligence.com/industry-reports/chitosan-market.

10 M. Hussain, *et al.*, Fungal chitosan in focus: a comprehensive review on extraction methods and applications, *Food Res. Int.*, 2025, **220**, 117103, DOI: 10.1016/j.foodres.2025.117103.

11 S. Crognale, C. Russo, M. Petruccioli and A. D'Annibale, Chitosan production by fungi: current state of knowledge, future opportunities and constraints, *Fermentation*, 2022, **8**, 76, DOI: 10.3390/fermentation8020076.

12 J. Zhu, D. Tian, X. Chen, J. Cui and R. Gao, Development of Schiff base–type oleogels using the emulsion template approach at different pH values: comparative investigation of their structure and properties, *Curr. Res. Food Sci.*, 2025, **8**, 101202, DOI: 10.1016/j.crfs.2025.101202.

13 G. B. Brito, V. O. D. S. Peixoto, M. T. Martins, D. K. A. Rosário, J. N. Ract, C. A. Conte-Júnior, A. G. Torres and V. N. Castelo-Branco, Development of chitosan-based oleogels via crosslinking with vanillin using an emulsion templated approach: structural characterization and their application as fat-replacer, *Food Struct.*, 2022, **32**, 100264, DOI: 10.1016/j.foostr.2022.100264.

14 Á. Mosquera, L. Montes, C. A. Pena, M. López-Pedrouso, J. Sineiro and D. Franco, Chitosan–olive oil oleogels for food applications: physicochemical and functional properties, *Foods*, 2025, **14**, 3332, DOI: 10.3390/foods14193332.

15 M. Rinaudo, M. Milas and P. Le Dung, Characterization of chitosan: influence of ionic strength and degree of acetylation on chain expansion, *Int. J. Biol. Macromol.*, 1993, **15**, 281–285, DOI: 10.1016/0141-8130(93)90027-J.

16 L. Montes, M. Gisbert, I. Hinojosa, J. Sineiro and R. Moreira, Impact of drying on the sodium alginate obtained after polyphenols ultrasound-assisted extraction from *Ascophyllum nodosum* seaweeds, *Carbohydr. Polym.*, 2021, **272**, 118455, DOI: 10.1016/j.carbpol.2021.118455.

17 M. Lama, L. Montes, D. Franco, A. Franco-Uría and R. Moreira, Chitosan-based oleogels: emulsion drying kinetics and physical, rheological, and textural characteristics of olive oil oleogels, *Mar. Drugs*, 2024, **22**, 318, DOI: 10.3390/md22070318.

18 E. Morales, N. Iturra, I. Contardo, M. Quilaqueo, D. Franco and M. Rubilar, Fat replacers based on oleogelation of beeswax/shellac wax and healthy vegetable oils, *LWT–Food Sci. Technol.*, 2023, **185**, 115144, DOI: 10.1016/j.lwt.2023.115144.

19 L. Brühl, *Official Methods and Recommended Practices of the American Oil Chemists' Society*, AOCS Press, Champaign, IL, USA, 7th edn, 2017.

20 Q. Zhao, C. Selomulya, S. Wang, H. Xiong, X. D. Chen, W. Li, H. Peng, J. Xie, W. Sun and Q. Zhou, Enhancing the oxidative stability of food emulsions with rice dreg protein hydrolysate, *Food Res. Int.*, 2012, **48**, 876–888, DOI: 10.1016/j.foodres.2012.07.004.

21 A. Brodkorb, L. Egger, M. Alminger, P. Alvito, R. Assunção, S. Ballance, T. Bohn, C. Bourlieu-Lacanal, R. Boutrou, F. Carrière, *et al.*, INFOGEST static in vitro simulation of gastrointestinal food digestion, *Nat. Protoc.*, 2019, **14**, 991–1014, DOI: 10.1038/s41596-018-0119-1.

22 Y. Li and D. J. McClements, New mathematical model for interpreting pH-stat digestion profiles: impact of lipid droplet characteristics on in vitro digestibility, *J. Agric. Food Chem.*, 2010, **58**, 8085–8092, DOI: 10.1021/jf101325m.

23 M. P. M. da Costa, M. C. Delpech, I. L. de Mello Ferreira, M. T. de Macedo Cruz, J. A. Castanharo and M. D. Cruz, Evaluation of single-point equations to determine intrinsic viscosity of sodium alginate and chitosan with high deacetylation degree, *Polym. Test.*, 2017, **63**, 427–433, DOI: 10.1016/j.polymertesting.2017.09.003.

24 A. Dodero, S. Vicini, M. Alloisio and M. Castellano, Rheological properties of sodium alginate solutions in the presence of added salt: an application of Kulicke equation, *Rheol. Acta*, 2020, **59**, 365–374, DOI: 10.1007/s00397-020-01206-8.
25 R. F. Fedors, An equation suitable for describing the viscosity of dilute to moderately concentrated polymer solutions, *Polymer*, 1979, **20**, 225–228, DOI: 10.1016/0032-3861(79)90226-X.
26 T. Sannan, K. Kurita and Y. Iwakura, Studies on chitin, 2. Effect of deacetylation on solubility, *Makromol. Chem.*, 1976, **177**, 3589–3600, DOI: 10.1002/macp.1976.021771210.
27 C. K. S. Pillai, W. Paul and C. P. Sharma, Chitin and chitosan polymers: chemistry, solubility and fiber formation, *Prog. Polym. Sci.*, 2009, **34**, 641–678, DOI: 10.1016/j.progpolymsci.2009.04.001.
28 C. Qin, Y. Du, L. Xiao, Z. Li and X. Gao, Enzymic preparation of water-soluble chitosan and their antitumor activity, *Int. J. Biol. Macromol.*, 2002, **31**, 111–117, DOI: 10.1016/S0141-8130(02)00064-8.
29 H. Karaer and İ. Kaya, Synthesis, characterization, and thermal decompositions of Schiff base polymers containing chitosan unit, *Iran. Polym. J.*, 2015, **24**, 471–480, DOI: 10.1007/s13726-015-0338-z.
30 C. Xu, W. Zhan, X. Tang, F. Mo, L. Fu and B. Lin, Self-healing chitosan/vanillin hydrogels based on Schiff-base bond/hydrogen bond hybrid linkages, *Polym. Test.*, 2018, **66**, 155–163, DOI: 10.1016/j.polymertesting.2018.01.016.
31 L. Marin, B. Simionescu and M. Barboiu, Imino-chitosan biodynamers, *Chem. Commun.*, 2012, **48**, 8778–8780, DOI: 10.1039/c2cc34337a.
32 R. S. Jagadish, K. N. Divyashree, P. Viswanath, P. Srinivas and B. Raj, Preparation of N-vanillyl chitosan and 4-hydroxybenzyl chitosan and their physico-mechanical, optical, barrier, and antimicrobial properties, *Carbohydr. Polym.*, 2012, **87**, 110–116, DOI: 10.1016/j.carbpol.2011.07.024.
33 S. Mun, E. A. Decker and D. J. McClements, Effect of molecular weight and degree of deacetylation of chitosan on the formation of oil-in-water emulsions stabilized by surfactant–chitosan membranes, *J. Colloid Interface Sci.*, 2006, **296**, 581–590, DOI: 10.1016/j.jcis.2005.09.023.
34 U. Klinkesorn, The role of chitosan in emulsion formation and stabilization, *Food Rev. Int.*, 2013, **29**, 371–393, DOI: 10.1080/87559129.2013.818013.
35 L. Payet and E. M. Terentjev, Emulsification and stabilization mechanisms of O/W emulsions in the presence of chitosan, *Langmuir*, 2008, **24**, 12247–12252, DOI: 10.1021/la8019217.
36 J. Zhang, Z. Guo, Y. Zhu, Y. Liu, X. Li, Q. Zhang and X. Liu, Ultrastable water-in-oil high internal phase emulsions featuring interfacial and biphasic network stabilization, *ACS Appl. Mater. Interfaces*, 2019, **11**, 28823–28830, DOI: 10.1021/acsami.9b05089.
37 N. Calero, J. Muñoz, P. W. Cox, A. Heuer and A. Guerrero, Influence of chitosan concentration on the stability, microstructure and rheological properties of O/W emulsions formulated with high-oleic sunflower oil and potato protein, *Food Hydrocoll.*, 2013, **30**, 152–162, DOI: 10.1016/j.foodhyd.2012.05.004.
38 Z. Xi, W. Liu, D. J. McClements and L. Zou, Rheological, structural, and microstructural properties of ethanol-induced cold-set whey protein emulsion gels: effect of oil content, *Food Chem.*, 2019, **291**, 22–29, DOI: 10.1016/j.foodchem.2019.04.011.
39 A. Y. Malkin, I. Masalova, P. Slatter and V. Verzhbitsky, Effect of droplet size on the rheological properties of highly concentrated W/O emulsions, *Rheol. Acta*, 2004, **43**, 584–591, DOI: 10.1007/s00397-003-0347-2.
40 M. Espert, I. Hernando, E. Llorca, A. Quiles and A. Salvador, Rheological properties of emulsion templated oleogels based on xanthan gum and different structuring agents, *Curr. Res. Food Sci.*, 2022, **5**, 564–570, DOI: 10.1016/j.crfs.2022.03.001.
41 O. Diez-Sales, M. Dolz, M. J. Hernández, A. Casanovas and M. Herráez, Rheological characterization of chitosan matrices: influence of biopolymer concentration, *J. Appl. Polym. Sci.*, 2007, **105**, 2121–2128, DOI: 10.1002/app.25577.
42 W. Miao, D. J. McClements, J. Han, H. Ji, Z. Jin and C. Qiu, Enhancement of rheological properties and oxidative stability of OSA starch oleogels by chitosan–EGCG conjugates: influence of chitosan viscosity, *Food Hydrocoll.*, 2026, **172**, 112027, DOI: 10.1016/j.foodhyd.2025.112027.
43 K. Enoch, C. S. Rakavi and A. A. Somasundaram, Thixotropic chitosan hydrogels for biomedical applications: unravelling the effect of chitosan concentration on the mechanical behaviour, *Surf. Interfaces*, 2024, **50**, 104475, DOI: 10.1016/j.surfin.2024.104475.
44 L. P. Barragán-Martínez, L. Alvarez-Poblano, E. J. Vernon-Carter and J. Alvarez-Ramírez, Effects of β-carotene on the color, textural, rheological and structural properties of canola oil/beeswax oleogel, *J. Food Meas. Char.*, 2022, **16**, 3946–3956, DOI: 10.1007/s11694-022-01449-4.
45 J. Zhu, D. Tian, X. Chen, T. Huang and X. Chen, Preparation of chitosan-phenolic aldehyde fragrance oleogels and comparative study of their structure and properties, *Food Bioprocess Technol.*, 2024, **17**, 4204–4214, DOI: 10.1007/s11947-024-03390-4.
46 C. Park, O. Campanella and F. Maleky, The effects of whey protein and oleogel interactions on mechanical properties of oleocolloids and hydro-oleocolloids matrices, *Food Hydrocoll.*, 2022, **124**, 107285, DOI: 10.1016/j.foodhyd.2021.107285.
47 M. Ziarno, D. Derewiaka, A. Florowska and I. Szymańska, Comparison of the spreadability of butter and butter substitutes, *Appl. Sci.*, 2023, **13**, 2600, DOI: 10.3390/app13042600.
48 M. Županjac, D. Ubiparip, P. Ikonić and M. Pojić, Next-generation spreads: emerging trends and innovation, *Future Foods*, 2025, 100821, DOI: 10.1016/j.fufo.2025.100821.
49 European Commission, *Commission Regulation (EU) Amending Regulation (EEC) No 2568/91 on the Characteristics of Olive Oil and Olive-Residue Oil and on the Relevant*

Methods of Analysis (No 61/2011 of 24 January 2011), European Commission, Brussel, Belgium, 2011.

50 K. W. Kim and R. L. Thomas, Antioxidative activity of chitosans with varying molecular weights, *Food Chem.*, 2007, **101**, 308–313, DOI: 10.1016/j.foodchem.2006.01.038.

51 O. G. Bountagkidou, S. A. Ordoudi and M. Z. Tsimidou, Structure–antioxidant activity relationship study of natural hydroxybenzaldehydes using in vitro assays, *Food Res. Int.*, 2010, **43**, 2014–2019, DOI: 10.1016/j.foodres.2010.05.021.

52 K. L. May, K. J. Tangso, A. Hawley, B. J. Boyd and A. J. Clulow, Interaction of chitosan-based dietary supplements with fats during lipid digestion, *Food Hydrocoll.*, 2020, **108**, 105965, DOI: 10.1016/j.foodhyd.2020.105965.

53 J. Zhang, R. Zhang, P. Wang, P. Wen, W. Zhang, S. Liu and F. Ren, Impact of chitosan on lipid digestion under simulated gastro-intestinal conditions, *Food Chem.:X*, 2025, 103014, DOI: 10.1016/j.fochx.2025.103014.

54 M. Golding and T. J. Wooster, The influence of emulsion structure and stability on lipid digestion, *Curr. Opin. Colloid Interface Sci.*, 2010, **15**, 90–101, DOI: 10.1016/j.cocis.2009.11.006.

55 E. Malinauskytė, J. Ramanauskaitė, M. Keršienė, I. Jasutienė, D. Leskauskaitė, T. G. Devold and G. E. Vegarud, Impact of interfacial composition on emulsion digestion using in vitro and in vivo models, *J. Food Sci.*, 2018, **83**, 2850–2857, DOI: 10.1111/1750-3841.14360.